Materials Chemistry and Physics 129 (2011) 228–235

Contents lists available at ScienceDirect

Materials Chemistry and Physics

journal homepage: www.elsevier.com/locate/matchemphys

Crosslinking chemistry of curing carbon composites containing novolac/furfuryl alcohol resins and carbon black or mesophase pitch as additives

Xiaoqing Zhang[a,*], Sarah Khor[a], Dachao Gao[a], Elaine Sum[b]

[a] CSIRO Materials Science and Engineering, Private Bag 33, Clayton South, Victoria 3169, Australia
[b] Technology and R&D, Rio Tinto Alcan, Aluval, 725 Rue Aristide Berges, 3834 Voreppe, France

ARTICLE INFO

Article history:
Received 11 January 2011
Received in revised form 30 March 2011
Accepted 31 March 2011

Keywords:
Crosslinking chemistry
Carbon composites
Polymer binders
Solid-state NMR

ABSTRACT

The crosslinking chemistry was studied for producing carbon composites using carbon black or mesophase pitch as additives and a binder containing novolac and furfuryl alcohol (FA) resins and hexamethylene tetramine (HMTA) as a crosslinker. Curing the composites to 205 °C generated FA, water and ammonia as the major volatile species released from the systems due to evaporation, condensation of FA and crosslinking reactions between the resins and HMTA, respectively. Carbon black or mesophase displayed a minimal effect on the chemical nature of the volatiles released from the curing. However, the carbon black particles, which were homogeneously distributed in the cured composite, produced a broad distribution of chemical environments and structures of the binder networks, and the chain motions of the binder were also modified. Mesophase pitch on the other hand was likely to participate in curing reactions of the resin phase and heterogeneous phase structures were detected only on a scale as small as ~2 nm in the composite.

1. Introduction

As the initial synthetic resins developed over a century ago, phenolic and furfuryl alcohol (FA) resins have been commercially used in varies applications from commodity and construction materials to high technology industries due to its characteristic properties such as excellent mechanical strength, dimensional stability, solvent resistance and flame retardance. The chemistry and applications of these resins has been studied over several decades [1–7]. Comprehensive research has been conducted to investigate the curing and baking chemistry for phenolic and FA resins by using model compounds and commercial resins. ^{13}C and/or ^{15}N enriched crosslinkers such as formaldehyde or hexamethylene tetramine (HMTA) were also used to enhance the signals derived from the crosslinkers which made it possible to detect various intermediate structures formed during the crosslinking reactions and thus identify the reaction pathway of the resins [8–21].

When novolac and FA resins are combined in application as a binding agent, liquid FA can act as a solvent for solid novolac where the viscosity of the binder system can be controlled by varying the amount of FA, therefore, processing and mechanical performance can be greatly improved especially when the system is used to fabricate carbon composites, reduction composites and refractories in the metal industries. The binder resins would also form amorphous carbon eventually upon heating to high temperatures with high carbon yield. However, when the resins are used in fabricate carbon composites, the carbon additives should also play a role in the crosslinking and carbonization reactions due to interactions between the resins and the carbon additives. Some carbon additives may also participate in the reactions during the curing or baking at high temperatures, thus, the reaction pathways, the reactivity and morphology of the final carbon composites will be significantly varied. Understanding the chemistry and the morphology behaviour along with the curing and baking process for these systems are fundamentally important to design/modify the performance of the carbon composites, but this has not been investigated thoroughly.

The inter-reaction pathways of the novolac/HMTA/FA mixing systems and the formation of highly crosslinked polymer networks containing both phenol and furan rings were reported in conjunction with the carbonization chemistry of the resin systems [22,23]. Leveraging the methodologies and knowledge gained from these previous studies on resin-only systems, we have conducted research on curing and baking carbon composites using novolac/HMTA/FA resins as the binder with carbon black and mesophase pitch as carbon additives. Carbon black is commonly used as additives to modify the mechanical and binding/processing performance of carbon composites, while mesophase pitch is an important precursor to produce advanced carbon composites with the capability to develop extended graphitic crystallinity [24–29]. Crosslinking chemistry of these carbon composites during curing process up to 205 °C was studied and reported in this paper, to explore the chemical nature of the volatiles released during the

* Corresponding author. Tel.: +61 3 95452653; fax: +61 3 95441128.
E-mail address: Xiaoqing.Zhang@csiro.au (X. Zhang).

0254-0584/$ – see front matter © 2011 Elsevier B.V. All rights reserved.
doi:10.1016/j.matchemphys.2011.03.084

curing, reaction pathways and structures formed in the solid phase of the cured composites. ^{13}C- and ^{15}N-enriched HMTA was used as a crosslinker in the binder phase and the results were compared to those of binder-only system for understanding the factors derived from carbon black or mesophase additives. The study of carbonization process of these carbon composites and thereafter the significantly different performance of these carbon materials will be published on later dates.

2. Experimental

2.1. Raw materials and sample preparation

Novolac resin (Resinox GC 1848), hexamethylene tetramine (HMTA) and furfuryl alcohol (FA: UCAR C34) were obtained from Huntsman Chemical Australia, Merck Pty., Ltd., and Orica Australia, respectively. Carbon black and mesophase pitch (AR Resin MP-P) were supplied by CanCarb Ltd., Canada and Mitsubishi Gas Chemical Company Inc. Carbon black aggregates were crush into small particles by a blender just before use. The obtained synthetic mesophase pitch sample was derived from naphthalene with particle size D [3,4] of 24.9 μm and softening point of 275–295 °C. All raw materials were used as received without purification or any further treatment.

The formulations of the novolac/HMTA/FA binder and composite samples are listed in Table 1. Solid novolac and HMTA were dissolved in FA liquid under mechanical stirring at a speed of 1050 rpm in a water bath (maintained at room temperature to avoid temperature increase during mixing which could cause curing) over 3 h to achieve a homogenous liquid binder (NHF-R). Carbon black or mesophase was then mixed with the NHF-R binder in a high speed mixer at a speed of 3000 rpm for 2–3 min to produce carbon black (NHF-C) or mesophase pitch (NHF-M) green composite samples. These samples were then cured on a small scale (3–5 g) in glass vials placed in a Memmert oven with a Eurotherm programming controller following a slow curing cycle (Table 2) up to 205 °C/4 h. The weight losses of the cured samples collected along the curing process at different curing temperatures were measured after cooling down to room temperature.

2.2. Characterization techniques

The fracture surface of the cured composite samples was examined by Philips FEI XL-30 SFEG scanning electron microscopy (SEM). The samples were mounted onto SEM stages with double-sided conductive tape and then sputter coated with gold of 20 nm thickness under argon atmosphere. The electron beam with an accelerating voltage of 5 kV was used to produce high definition images.

Thermogravimetric analysis Fourier transform infrared spectroscopy (TGA–FTIR) results were acquired using a TA SDT Q Series Explorer (Q600) TGA connected to a Nicolet Nexus 670 IR Spectrometer in inert atmosphere (nitrogen gas). A small amount of each green composite sample (~30 mg) was placed in the TGA sample pan and heated following an accelerated curing cycle (listed in Table 2) to 205 °C then held isothermally for 5 min. Volatiles generated from heating samples in the TGA furnace were transferred through the interface into the FTIR spectrometer maintained at 180 °C. Infra-red spectra were acquired continuously during the measurement with KBr Beam splitter, resolution of 4 cm^{-1} and 365 scans for each spectrum.

In order to enhance the nuclear magnetic resonance (NMR) signals derived from HMTA, ^{13}C and ^{15}N, 97–98% enriched HMTA (synthesized by Sigma–Aldrich as requested) was used instead of conventional HMTA to prepare the samples for high-resolution solid-state NMR experiments following the same sample mixing and curing procedures. All NMR measurements were conducted at room temperatures using a Varian NMR300 System at resonance frequencies of 75 MHz for carbon-13 and 30 MHz for nitrogen-15 under conditions of cross polarization (CP), magic angle sample spinning (MAS) and high-power dipolar decoupling (DD). The 90° pulse-width was of 5.8 μs while the contact time was 1 ms. The rate of MAS was at a value around 7–8 kHz and no spinning side band was observed for ^{15}N spectra when using such a MAS rate. The chemical shift of ^{13}C spectra was determined by taking the adamantine peak at up-field (29.5 ppm relative to TMS) as an external reference standard. For ^{15}N spectra, the enriched HMTA resonance at 44 ppm [18] was taken as an external reference. ^{1}H spin–lattice (T_1) and spin–lattice relaxation times in the rotating frame ($T_{1\rho}$) were measured via ^{13}C resonances using pulse sequences reported previously [30]. Solution NMR spectra were also measured using the same spectrometer with 10 mm solution probe head.

3. Results and discussion

3.1. Chemical nature of the volatiles released from the curing

The weight loss data during the curing of the NHF-R, NHF-C and -M systems are shown in Fig. 1, reflecting the volatile released during the curing. The weight loss up to 90 °C were minimal for all samples, however, it increased rapidly when the curing temperature was increased. After curing to 205 °C for a total of 35 h, NHF-R (resin-only sample) produced 19% of weight loss, while NHF-C and -M (containing 63% of resins) generated 13–14% weight loss (corresponding to 21–22% resin loss when assuming no volatile release from carbon black or mesophase pitch).

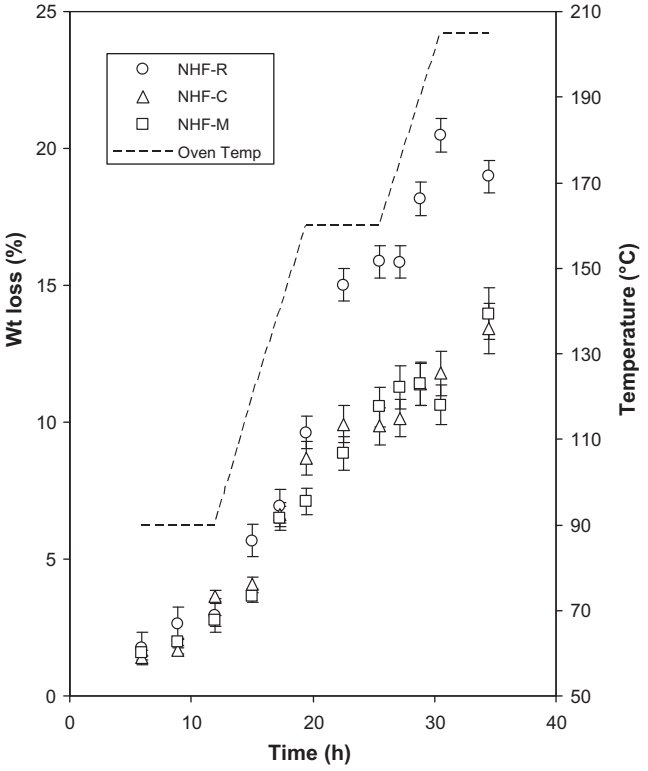

Fig. 1. Weight loss of NHF-R, -C and -M systems after curing to 205 °C/4 h.

TGA–FTIR measurement was conducted to examine the chemical nature of the volatiles released during the curing process. Due to the small scale testing for TGA analysis where only up to 30 mg samples could be packed into the TGA sample pan, a fast curing cycle listed in Table 2 was used to enhance the IR signal; all target temperatures remained the same as those used in oven curing, but

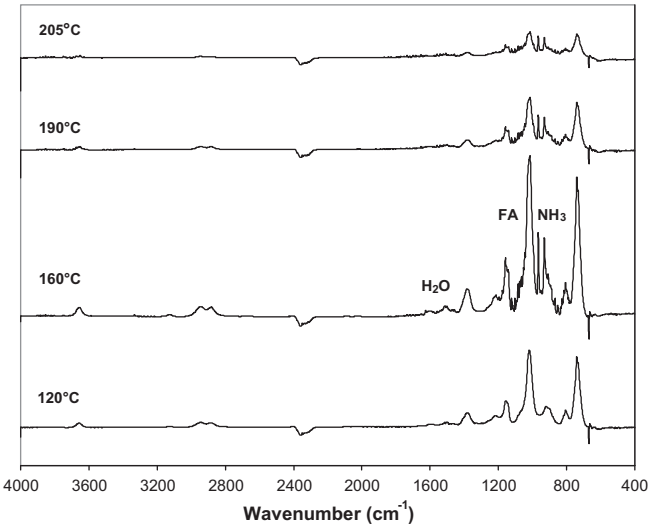

Fig. 2. FTIR spectra of volatiles collected at 120, 160, 190 and 205 °C/4 h during TGA testing for NHF-R sample.

Table 1
Formulations of the carbon composites (in weight parts).

Samples	Novolac	HMTA	FA	Carbons
NHF-R	24	5	34	0
NHF-C	24	5	34	37 (carbon black)
NHF-M	24	5	34	37 (mesophase pitch)

Table 2
Curing program.

Steps	Oven curing			TGA		
	1	2	3	1	2	3
Ramp (°C/h)	4.5	9	9	300	300	300
Temperature (°C)	90	160	205	90	160	205
Dwell time (min)	360	360	240	10	10	10

Table 3
Weight loss observed by oven curing or TGA after curing to 205 °C[a].

Samples	Wt loss (wt%) in oven curing	Resin loss (wt%) in oven curing	Wt loss (wt%) in TGA (%)	Resin loss (wt%) in TGA (%)
NHF-R	19.0	19.0	29.1	29.1
NHF-C	13.4	21.3	13.9	22.1
NHF-M	14.0	22.3	16.1	26.6

[a] Data error of 5–8%.

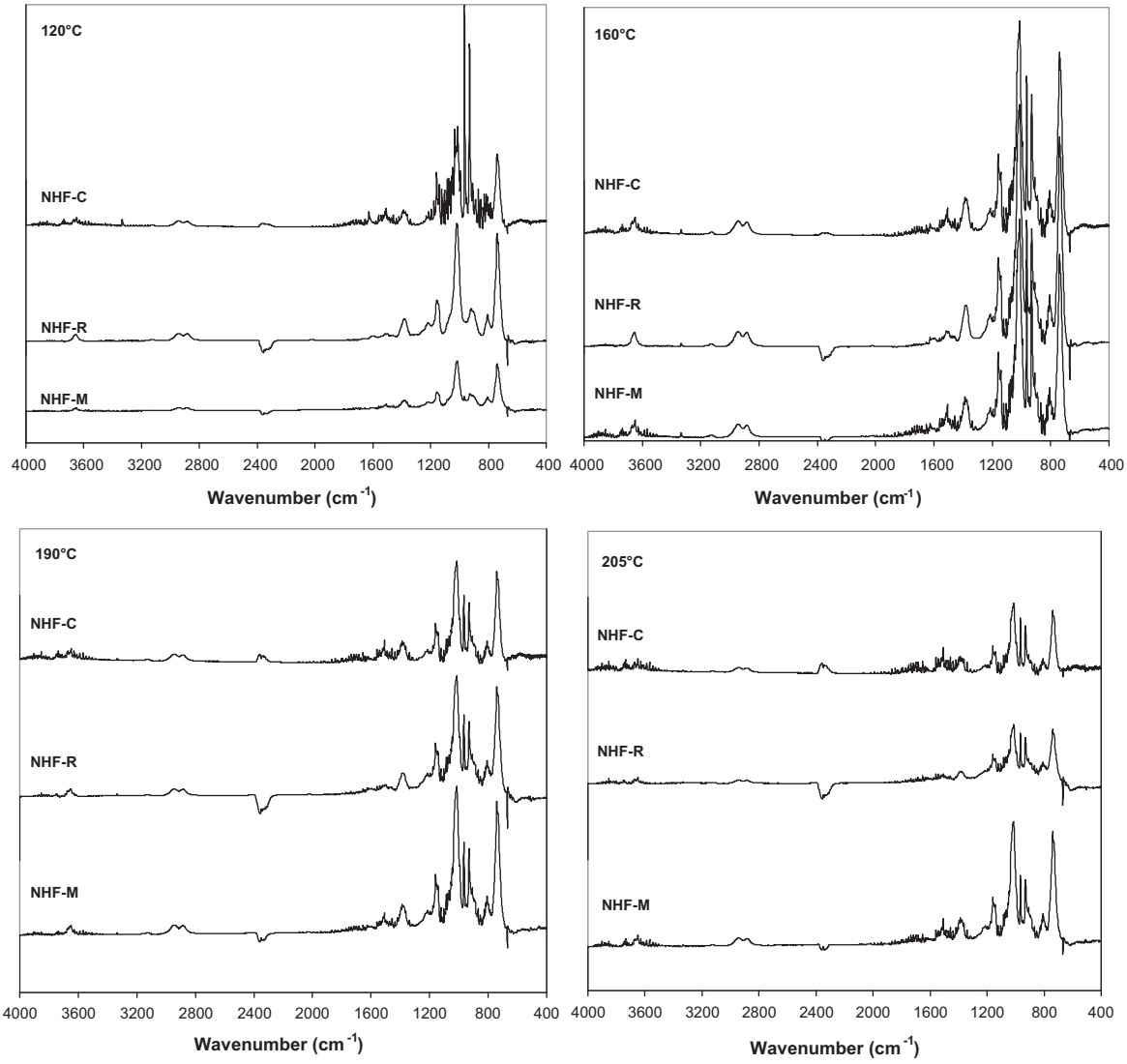

Fig. 3. FTIR spectra of the volatiles released during the curing process of NHF-R, -C and -M systems up to 205 °C/4 h.

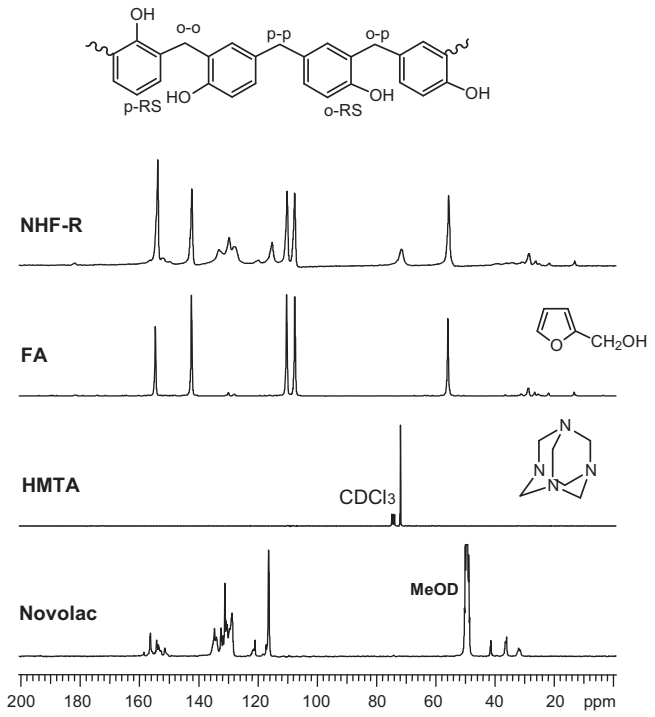

Fig. 4. ^{13}C solution NMR spectra of novolac, HMTA, FA and NHF-R before curing.

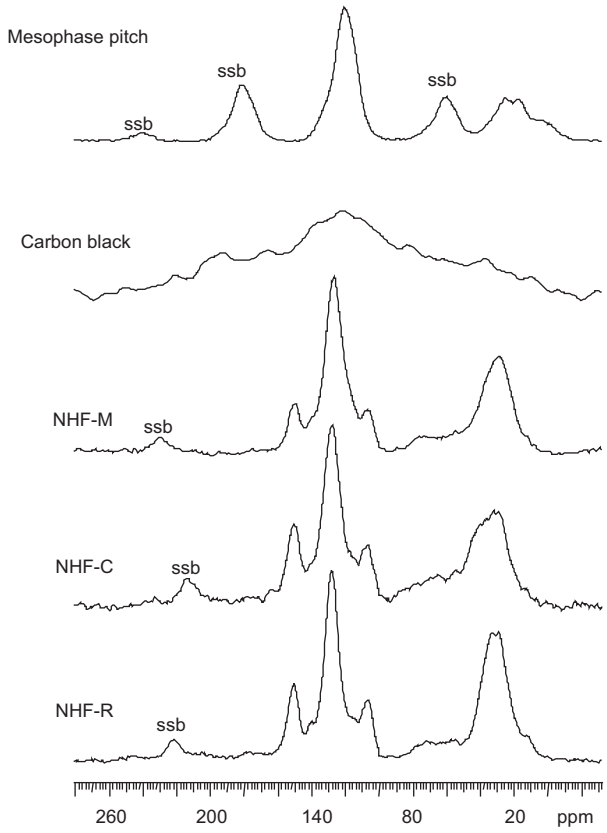

Fig. 5. ^{13}C CP/MAS NMR spectra of carbon black and mesophase pitch additives and those of NHF-R, -M, -C after curing to 205 °C/4 h (ssb: spinning-side band).

the heating rates or dwell times were ~35 times faster or shorter, thus the whole curing cycle up to 205 °C was completed within 1 h instead of 35 h in the oven curing. The weight loss data observed by this TGA method were compared with those obtained in the oven curing (35 h cycle with 3–5 g of samples) in Table 3. The resin loss data were calculated assuming all weight loss was derived only from the NHF-R binder. Note that the weight loss of NHF-R observed in TGA testing was higher than those obtained from the oven curing but the composite samples (NHF-C and -M) displayed similar data in both measurements.

The volatiles generated during the TGA testing were transferred into FTIR spectrometer and typical FTIR spectra observed at 120, 160, 190 and finally 205 °C are shown in Fig. 2. The observed FTIR spectra were compared with standard library spectra available in the spectrometer software to determine the chemical nature of the major products detected during the curing. At 120 °C, the major products were FA and a small amount of water. When temperature increased to 160 °C, the intensity of these signals was enhanced and signals characteristic to NH_3 were also detected. All of these signals were retained as the major components in the volatiles when the temperature was further increased to 190 and 205 °C, but their relative intensities were reduced.

The profiles of NHF-C and -M detected during the TGA–FTIR testing were similar to those observed for NHF-R as shown in Fig. 3, indicating the same varieties of volatiles were predominantly released from their resin phase. Carbon black or mesophase pitch did not significantly change the chemical nature of the volatiles.

3.2. Curing chemistry of the carbon composites

^{13}C solution NMR spectra of novolac (in deuterated methanol), HMTA (in deuterated chloroform), FA and NHF-R (no solvent) are shown in Fig. 4. The resonances of phenolic rings of novolac were displayed over a range of 110–160 ppm, and methylene linkages between phenolic rings located at a range of 29–43 ppm corresponding to *ortho–ortho* (29 ppm, 22%), *ortho–para* (35 ppm, 47%) and *para–para* (43 ppm, 31%) $-CH_2-$ linkages as determined by a method reported previously [18]. The vacant *ortho* or *para* phenolic reactive sites appeared at 116 and 121 ppm. A number-averaged phenolic unit number (5.35) was calculated via the ratio of aromatic (excluding Ar–O**H**) and aliphatic protons determined in ^1H solution NMR spectrum (not shown) using the same method as reported previously [18]. Only a single resonance at 44 ppm was detected for HMTA indicating hydrolysis of the compound had not occurred [18]. Five strong resonances were observed for FA corresponding to the structure as assigned previously [19]. The minor resonances over a broad range are due to the soap additives (~5%) as surfactants. The linewidth in the spectrum of NHF-R became broad due to the high viscosity of the liquid binder but no observable reaction occurred during the mixing process.

A very broad ^{13}C signal was observed in the CP/MAS NMR spectrum (Fig. 5) for carbon black due to its high C/H atomic ratio causing weak efficiency in cross polarization and decoupling. The mesophase pitch displayed a relatively narrow linewidth in the CP/MAS spectrum (Fig. 5) with aromatic resonances at 122 ppm and aliphatic resonances at 10–40 ppm which are consistent with reports in literature [26,29]. Cured NHF-R sample (Fig. 5) displayed aromatic phenolic/furfuryl resonances at 110–155 ppm and various aliphatic linkages between these phenolic/furfuryl rings around 20–80 ppm. The peak at 15 ppm was due to the methyl groups associated to the phenolic/furfuryl rings. These results are consistent with those reported previously [18,19,22]. The spectra of the cured NHF-C and -M were similar to that of NHF-R as shown in Fig. 5.

A large group of intermediate structures in the crosslinking novolac–furfuryl alcohol resins by HMTA has been reported in literature with reaction pathways postulated [18–20,22]. High-resolution solid-state NMR was applied here to study the curing reactions of the three systems. The greatly enhanced signals achieved by using $^{13}C/^{15}N$ enriched HMTA made it possible to

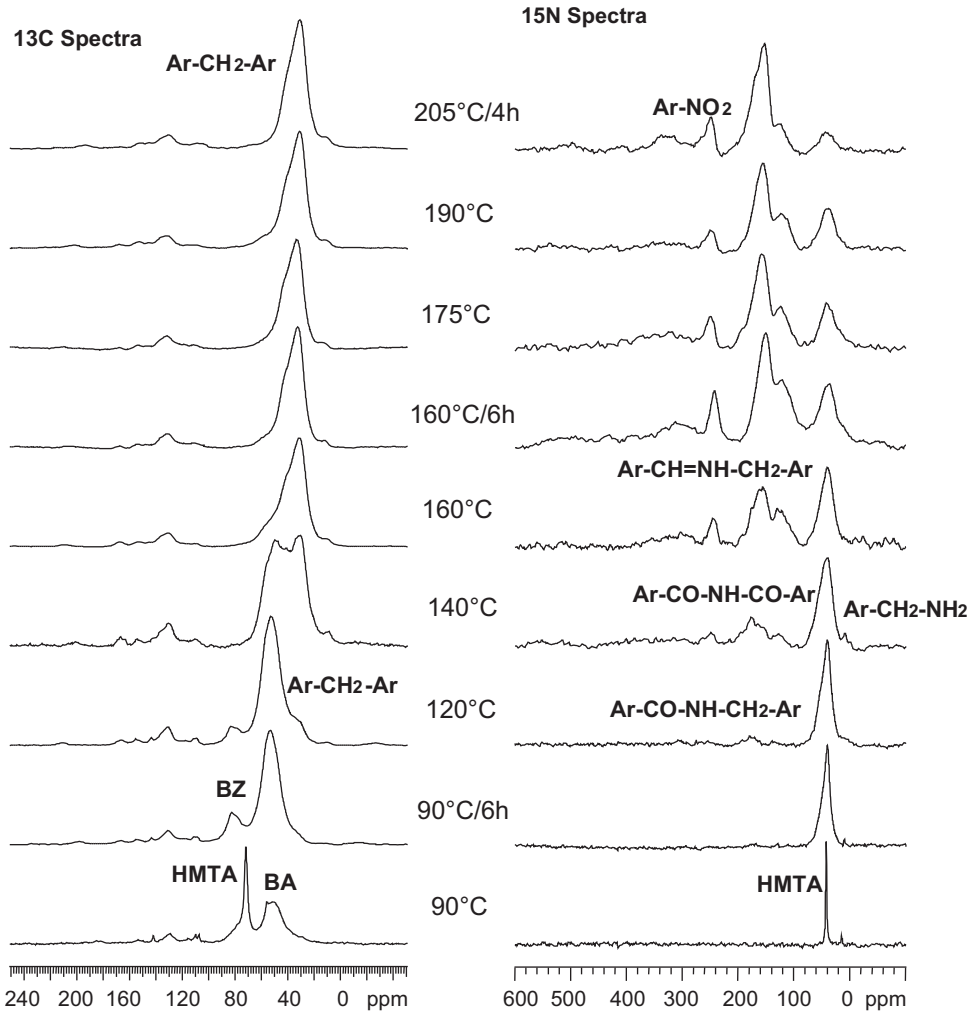

Fig. 6. ^{13}C and ^{15}N CP/MAS NMR spectra of NHF-R cured to various temperatures up to 205 °C/4 h.

examine the effect of additives on structures formed during the curing in detail. Fig. 6 shows ^{13}C and ^{15}N CP/MAS NMR spectra of NHF-R cured to different temperatures. After curing to 90 °C, the HMTA resonances were still observed at 74 ppm in the ^{13}C spectrum and at 44 ppm in the ^{15}N spectrum. New resonances at 50–55 ppm in the ^{13}C spectrum were detected corresponding to the formation of tri- and di-benzylamine (BA) intermediates. Minor resonances at 3–5 ppm in the ^{15}N spectrum were attributed to the formation of CH_3NH_2 or NH_3 broken from the HMTA. After curing to 90 °C for 6 h, the narrow signal of HMTA disappeared in both ^{13}C and ^{15}N spectra and new resonances at 82 and 50–60 ppm in ^{13}C spectrum were detected corresponding to the formation of benzoxazine (BZ) as well as BA, respectively. The broad peak at 48 ppm in ^{15}N spectrum was consistent with this result. A further increase in the curing temperature resulted in the formation of amide and imide structures with resonances observed at 162 ppm in ^{13}C spectra and at 90–150 ppm in ^{15}N spectra. These intensities increased as curing temperatures increased. A shoulder peak at 30–35 ppm in ^{13}C spectra was observed simultaneously after curing to 120 °C, and its intensity increased significantly as curing temperature increased, corresponding to the formation of methylene linkages between phenol/furan rings. At the same time, intensities of resonances at 82, 50–60 ppm in ^{13}C spectra decreased and the 48 ppm peak in ^{15}N spectra shifted to 38 ppm due to the decomposition of BZ and BA intermediates and the formation of benzylammonium ions. Above 160 °C, the methylene intensity at 30 ppm in ^{13}C spectra was dominant until the end of curing, indicating that methylenes derived from HMTA were the major linkages in the finally cured resins. Nitrogen-containing structures (shown in ^{15}N spectra) such as amides (110–120 ppm), imides (140–160 ppm), nitriles (CN, at 260 ppm), imines (280–320 ppm), $-NO_2$ (350 ppm) and residual amines and benzylammonium ions (broad peaks at 30–40 ppm) were also formed during the curing process, and many of them retained in the final crosslinked networks. Methyl groups attached to phenol rings (~15 ppm in ^{13}C spectra) formed above 140 °C were also retained in the final resins. As reported previously [22], FA took part in the curing reactions between novolac/HMTA and their intermediates formed in the curing reaction to generate methylene linkages between phenol and furan rings, thus resulting in highly crosslinked networks. Similar nitrogen-containing structures such as amine, amide, imide, imine, CN and NO_2 structures were also formed between phenol and furan, or furan–furan, phenol–phenol rings in the networks.

The curing processes of NHF-C and -M composites detected by ^{13}C and ^{15}N CP/MAS NMR spectra were compared with those of NHF-R as shown in Figs. 7 and 8. In general, the NHF-C and -M systems followed a similar curing reaction pathway as NHF-R and produced similar chemical structures including nitrogen-containing structures in the cured systems. Noticeable difference was obtained for NHF-C, where the linewidth of the ^{13}C CP/MAS spectra became significantly broad. This could be caused by the formation of a broad distribution of chemical environments in the

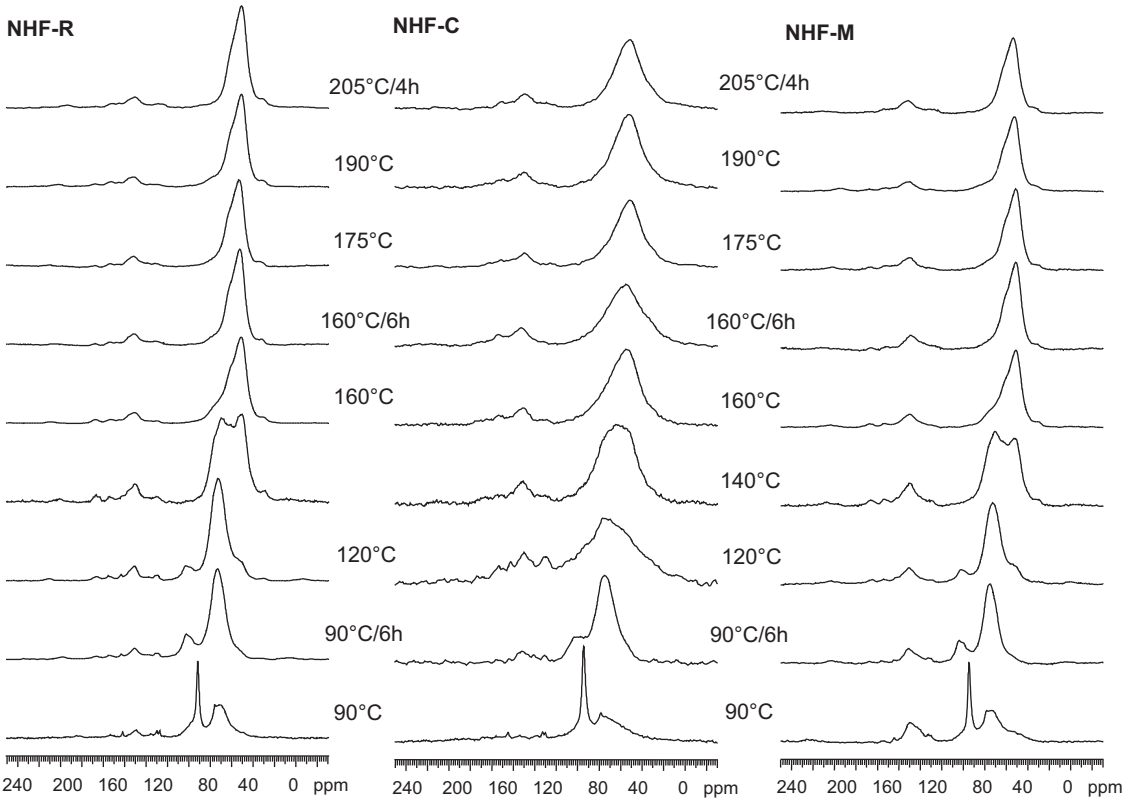

Fig. 7. ^{13}C CP/MAS NMR spectra of cured NHF-R, NHF-C and NHF-M systems.

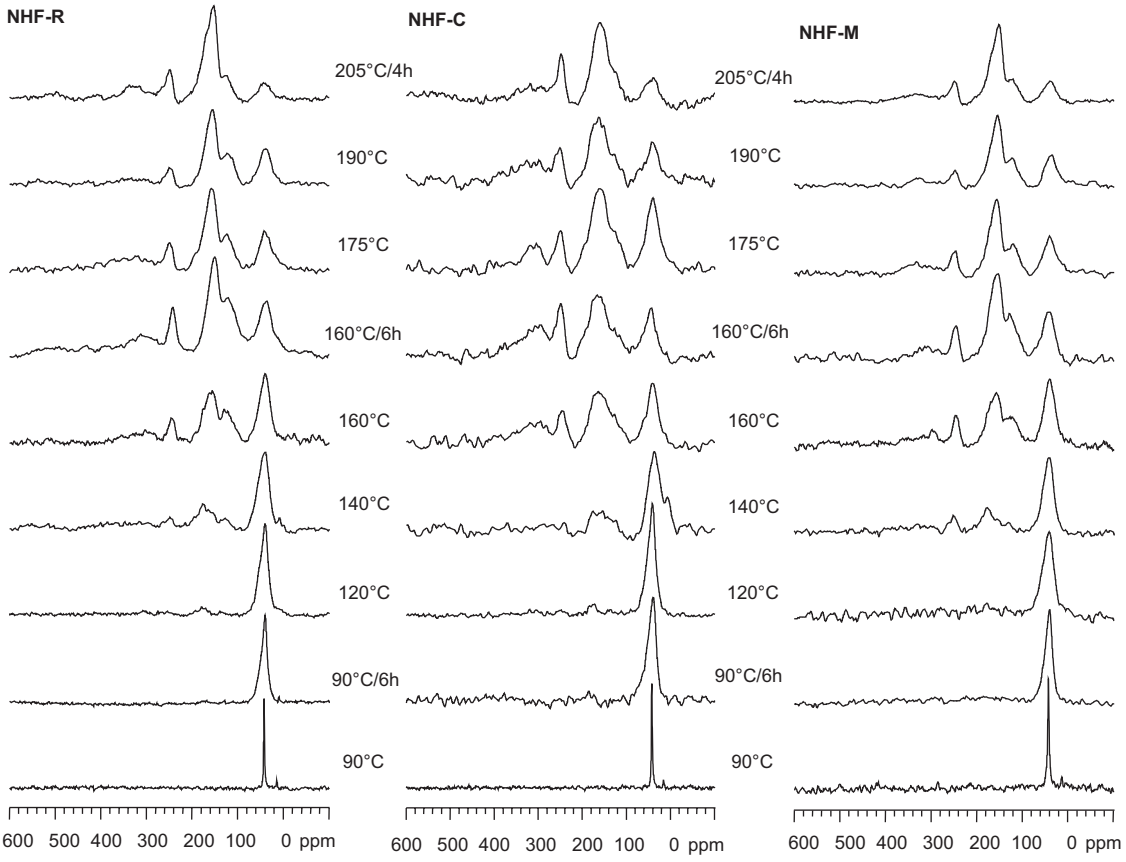

Fig. 8. ^{15}N CP/MAS NMR spectra of cured NHF-R, NHF-C and NHF-M systems.

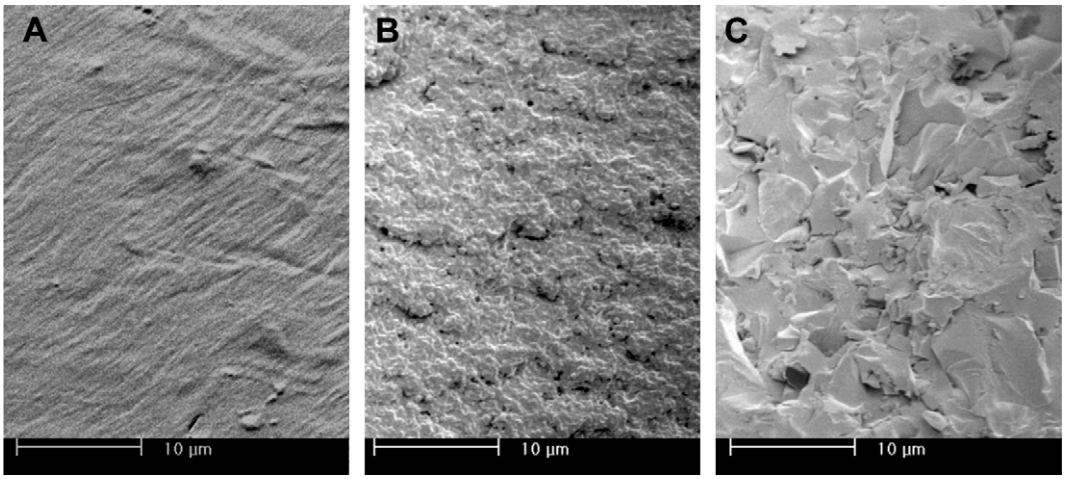

Fig. 9. SEM images of the fracture surfaces of NHF-R (A), NHF-C (B) and NHF-M (C) samples after curing to 205 °C/4 h.

binder due to the existence of carbon black in the curing system. The mobility decrease of the binder segments due to strong interactions between the resin segments and carbon black particles could also broaden the linewidth of ^{13}C spectra. However, the linewidth broadening in ^{15}N spectra of NHF-C samples was minimal and only occurred at higher temperatures, suggesting that those nitrogen-containing structures were not directly involved in the interactions with carbon black additives, possibly due to their hydrophilic nature (rather than hydrophobic), and the long chain mobility of the cured resins was also not varied significantly in NHF-C system.

3.3. Phase structures of the carbon composites after curing

The morphologies of NHF-R, -C and -M samples observed by SEM after curing to 205 °C are shown in Fig. 9. Amorphous morphology with smooth fracture surface was observed for the cured NHF-R sample while carbon black particles were homogeneously distributed in the binder phase in the NHF-C system. The cured NHF-M sample displayed a rough fracture surface but a continuous morphology of the whole NHF-M sample was obtained after curing. The mesophase pitch additives might either take part in the curing reaction with NHF-R or formed miscible morphologies phase with the cured binder phase. The phase structures of the cured composite systems were studied through examination of NMR relaxation behaviors.

Various molecular motions exist in polymer systems due to different chemical structures, different intra- and inter-molecular interactions and varied phase morphologies, which would be reflected in NMR relaxation parameters. The proton spin–lattice relaxation times (^1H T_1) and spin–lattice relaxation times in the rotating frame (^1H $T_{1\rho}$) are correlated to the molecular motions of polymer systems at MHz and kHz range, respectively. During the relaxation times, components with slow relaxation rates may be able to transfer the magnetization to fast relaxation components through spin–diffusion interaction when dipolar–dipolar interactions are strong in the system. This would result in averaging out of the relaxation rates among different components with different relaxation rates when domain size of the system is smaller than the effective spin–diffusion pathway during ^1H T_1 or $T_{1\rho}$ period (~20 nm or ~2 nm, respectively) [30–33]. Thus, the measurement of ^1H relaxation times also reflects the homogeneity/heterogeneity of multi-component systems.

^1H T_1 and $T_{1\rho}$ data of NHF-R, -C and -M systems after curing to 205 °C/4 h are listed in Table 4 (referring to Fig. 5) in conjunction with the data of mesophase before and after heating under the same condition to 205 °C/4 h. Single-component T_1 and $T_{1\rho}$ decays were observed via ^{13}C resonances of the cured NHF-R and the values observed through different resonances were also quite similar (Table 4). This indicates that the NHF-R crosslinked network system was homogeneous on nanometer scales; strong spin–diffusion interactions had averaged out the relaxation rates of both T_1 and $T_{1\rho}$ for difference components in the networks. The weak and broad signal of carbon black only appeared as base-line of the spectrum for cured NHF-C (Fig. 5), thus the observed resonances for NHF-C sample were only attributed to the NHF-R binder in the composite. Note that the T_1 data of the NHF-C were similar to those of NHF-R but their $T_{1\rho}$ values were slightly lower, suggesting a motional modification of the resins only occurred at kHz scales ($T_{1\rho}$ scale) due to interactions with the carbon black. The $T_{1\rho}$ data observed via the $-CH_2-$ resonances at 30 ppm for the NHF-R and -C samples using $^{13}C/^{15}N$ enriched HMTA (where the $-CH_2-$ resonances derived from HMTA was greatly enhanced) were also consistent with these results.

For the cured NHF-M sample, its T_1 also displayed a signal component with values similar to those for the NHF-R and -C, suggesting

Table 4
^1H T_1 and $T_{1\rho}$ data of cured NHF-R, -C and -M samples.

Samples	^1H T_1 (s)		^1H $T_{1\rho}$ (ms)		
	127 ppm	30–40 ppm	127 ppm	30–40 ppm	30 ppm[a]
NHF-R	1.03 ± 0.02	1.05 ± 0.02	6.4 ± 0.1	6.5 ± 0.2	6.7 ± 0.2
NHF-C	1.10 ± 0.01	1.08 ± 0.02	5.2 ± 0.1	5.2 ± 0.2	5.0 ± 0.1
NHF-M	1.11 ± 0.02	1.13 ± 0.03	2.2 ± 0.3 (47%)	2.4 ± 0.3 (46%)	2.2 ± 0.3 (17%)
			9.2 ± 0.7 (53%)	9.4 ± 0.8 (54%)	8.7 ± 0.4 (83%)
Mesophase pitch	0.90 ± 0.03	0.92 ± 0.04	4.2 ± 0.3	4.0 ± 0.2	–
Mesophase pitch 205 °C/4 h	0.33 ± 0.01	0.35 ± 0.02	0.64 ± 0.03	0.68 ± 0.07	–

[a] Date observed from the NHF samples using $^{13}C/^{15}N$ enriched HMTA.

a homogeneous system on ~20 nm scale. But the data were quite different from those of both cured and uncured mesophase-only samples (Table 4). Two $T_{1\rho}$ components were detected for the cured NHF-M sample and the values were similar for samples using either unlabeled HMTA or $^{13}C/^{15}N$ enriched HMTA. Note that the proportion of longer $T_{1\rho}$ component was much higher in the sample using $^{13}C/^{15}N$ enriched HMTA (where the signal of the resin was greatly enhanced), suggesting the existence of mesophase-rich (corresponding to the shorter $T_{1\rho}$ component) and resin-rich (with longer $T_{1\rho}$) phases. The whole cured NHF-M system was homogeneous on ~20 nm scales (identical T_1 values from different resonances) but heterogeneous on ~2 nm scales (multiple $T_{1\rho}$ components). The NHF-M system was immiscible before curing and normally the curing of the resin NHF phase would enhance the phase separation of such systems. The homogeneity on a scale of 20 nm for the cured NHF-M sample and the significant changes of the relaxation times of mesophase pitch in the cured NHF-M system are more likely due to formation of certain extend of chemical linkages between the mesophase pitch species and the NHF binder network under the curing condition, thus crosslinked network structures could be produced through the whole NHF-M system where NHF and mesophase pitch structures were intimately mixed. However, observation of direct evidence of formation of such covalent bonds is difficult for such highly crosslinked systems. On the other hand, the major interactions between the NHF network and the carbon black particles in NHF-C composite could be due to strong intermolecular interactions rather than chemical linkages via covalent bonds. Such difference in chemical/phase structures would produce different mechanical behaviour for the two carbon materials.

4. Conclusion

Curing the carbon composites containing novolac/FA/HMTA resins and carbon black or mesophase pitch as additives up to 205 °C generated FA, water and ammonia as the major volatile species due to evaporation, condensation of FA and crosslinking reactions with HMTA within the binder phase. The carbon black or mesophase additives displayed a minimal effect on the chemical nature of the volatile released. The composites also followed a similar curing reaction pathway to that of the NHF-R binder system and produced similar chemical structures containing various nitrogen-containing segments. However, the carbon black additives, which were homogeneously distributed in the binder, did produce a broad distribution of chemical environments and structures of the binder networks due to their strong interactions with the carbon black particles. The chain motions of the binder network on kHz scales were also modified. On the other hand, mesophase was likely to take part in the curing reactions of the binder and form crosslinked networks through the whole systems with homogeneous morphologies on ~20 nm scales. Phase structure heterogeneity was only detected on a scale as small as ~2 nm.

Acknowledgements

The authors are grateful to Dr. Shiqin Yan, Ms. Jennifer Peck and Mr. Robert Simmonds for their contribution in sample preparation and project discussion, and funding support from Rio Tinto Alcan.

References

[1] R.W. Martin, Chemistry of Phenolic Resins, Wiley, New York, 1956.
[2] A.P. Dunlop, F.N. Peters, The Furans, Reinhold, New York, 1953.
[3] N.J.L. Megson, Phenolic Resin Chemistry, Butterworths, London, 1958.
[4] A. Knop, W. Scheib, Chemistry and Application of Phenolic Resins, Springer-Verlag, 1979.
[5] A. Knop, L. Pilato, Phenolic Resins, Springer-Verlag, New York, 1979.
[6] A. Knop, L. Pilato, Phenolic Resins: Chemistry, Applications and Performance: Future Directions, Springer-Verlag, Berlin, 1985.
[7] L. Pilato, Phenolic Resins: A Century of Progress, Springer-Verlag, Berlin, Heidelberg, 2010.
[8] S.A. Sojka, R.A. Wolfe, E.D. Dietz Jr., B.F. Dannels, Macromolecules 12 (1979) 767.
[9] C.A. Fyfe, A. Rudin, W. Tchir, Macromolecules 13 (1980) 1320.
[10] S.A. Sojka, R.A. Wolfe, G.D. Guenther, Macromolecules 14 (1981) 1539.
[11] G.E. Maciel, I.S. Chuang, G.E. Myers, Macromolecules 15 (1982) 1218.
[12] C.A. Fyfe, M.S. McKinnon, A. Rudin, W.J. Tchir, Macromolecules 16 (1983) 1216.
[13] R.L. Bryson, G.R. Hatfield, T.A. Early, A.P. Palmer, G.E. Maciel, Macromolecules 16 (1983) 1669.
[14] G.E. Maciel, I.S. Chuang, L. Gollob, Macromolecules 17 (1984) 1081.
[15] G.R. Hatfield, G.E. Maciel, Macromolecules 20 (1987) 608.
[16] L.E. Bogan Jr., Macromolecules 24 (1991) 4807.
[17] A. Shindo, K. Izumino, Carbon 32 (1994) 1233.
[18] X. Zhang, M.G. Looney, D.H. Solomon, A.K. Whittaker, Polymer 38 (1997) 5835.
[19] X. Zhang, D.H. Solomon, J. Polym. Sci. Part B: Polym. Phys. 35 (1997) 2233.
[20] X. Zhang, D.H. Solomon, Polymer 39 (1998) 6153.
[21] A.S.C. Lim, D.H. Solomon, X. Zhang, J. Polym. Sci. Part A: Polym. Chem. 37 (1999) 1347.
[22] X. Zhang, D.H. Solomon, Chem. Mater. 10 (1998) 1833.
[23] X. Zhang, D.H. Solomon, Chem. Mater. 11 (1999) 384.
[24] K. Kanno, J.J. Fernandez, F. Fortin, Y. Korai, I. Mochida, Carbon 35 (1997) 1627.
[25] K.A. Trick, T.E. Saliba, Carbon 33 (1995) 1509.
[26] I. Mochida, Y. Korai, C.H. Ku, F. Watanabe, Y. Sakai, Carbon 38 (2000) 305.
[27] K. Kanno, N. Koike, Y. Korai, I. Mochida, M. Komatsu, Carbon 37 (1999) 195.
[28] M. Dumont, M.A. Dourges, X. Bourrat, R. Pailler, R. Naslain, O. Babot, M. Birot, J.P. Pillot, Carbon 43 (2005) 2277.
[29] K. Murakami, M. Okumura, M. Yamamoto, Y. Sanada, Carbon 34 (1996) 187.
[30] V.J. McBrierty, K. Packer, Nuclear Magnetic Resonance in Solid Polymers, Cambridge University Press, Cambridge, 1993.
[31] X. Zhang, K. Takegoshi, K. Hikichi, Macromolecules 24 (1991) 5756.
[32] X. Zhang, K. Takegoshi, K. Hikichi, Macromolecules 25 (1992) 2336.
[33] X. Zhang, D.H. Solomon, Macromolecules 27 (1994) 4919.